Engineering Solid Mechanics 9 (2021) 1-12

Contents lists available at GrowingScience

Engineering Solid Mechanics

homepage: www.GrowingScience.com/esm

Free vibrations of tapered shear deformable column

Byoung Koo Lee[a], Sang Jin Oh[b], Tae Eun Lee[c] and Gweon Sik Kim[a*]

[a]*Department of Civil and Environmental Engineering, Wonkwang University, 460 Iksan-daero, Iksan-si, Jeollabuk-do 54538, South Korea*
[b]*Department of Civil and Environmental Engineering, Jeonnam State University, 152 Jookrokwon-ro, Damyang-eup, Jeollanam-do, 57337, South Korea*
[c]*School of Architecture, Civil and Landscape Engineering, Donggang University, 50 Dongmoon-daero, Buk-gu, Kwangju-si, 61200, South Korea*

ARTICLEINFO

Article history:
Received 20 May 2020
Accepted 30 July 2020
Available online
30 July 2020

Keywords:
Free vibration
Tapered column
Shear deformation
Mode shape
Natural frequency

ABSTRACT

In this paper, free vibrations of the tapered shear deformable column are studied. The column is clamped at the bottom and is free or hinged or clamped at the top. The column has a tapered cross-section, square and circular, under the condition of constant volume. The axial compressive load is acted to the top. The differential equations of such column were derived, in which the effects of the rotary inertia and shear deformation were included. For computing natural frequencies with mode shapes, the differential equations were solved numerically. The effects of column parameters of the frequencies and mode shapes were performed, and its results were extensively discussed.

1. Introduction

Because the column is the most important structural unit, the dynamic problems, especially free vibrations, of elastic columns under the various considerations such as the end condition, cross-section, taper type, effects of rotary inertia, shear deformation and mechanical properties have been investigated in the past decades. Accurate computing of dynamic response, including the free vibration behaviors of the structures, is important for the structural design and stability analysis of structures acting the external dynamic loads. In the dynamic analysis of the structure, effects of both the rotary inertia and shear deformation could be either included or excluded. For example, all these effects are excluded in the ordinary beam theory, but all these effects are considered in the Timoshenko beam theory. These two theories generally yield natural frequencies that are not very different. However, in cases of short columns, composite columns and columns excited by high-frequencies, the Timoshenko beam theory is more effective in computing accurate frequencies (Timoshenko & Young, 1974). In this regard, many researchers, such as Shimpi et al. (2017), Lee et al. (2013), Viola et al. (2007), Loya et al. (2006), Yardimoglu and Yildirim (2004), Zhou (2000) and Takahashi (1999) have studied the free vibrations of the Timoshenko beams/columns.

* Corresponding author.
E-mail addresses: gskim1531@wku.ac.kr (G.S. Kim)

doi: 10.5267/j.esm.2020.8.001

In many infra structures built in the aerospace, architectural, civil and mechanical engineering, tapered members are often utilized for various reasons of geometric, aesthetic and economic issues. Structural analyses related to taper components have been performed by many researchers such as Lee and Lee (2020), Andrade et al. (2007), Yau (2006), Maalek (2004), Li and Li (2002) and Yang and Yau (1987). As mentioned above, the subject on Timoshenko beam with tapered component is attractive to structural engineers. Regarding past research trends, this paper studies free vibrations of the tapered shear deformable column, where both the rotary inertia and shear deformation effects are considered using the Timoshenko beam theory. There are three main topics in this study: (i) to derive the differential equations governing free vibrations of the tapered shear deformable column; (ii) to develop solution methods for computing natural frequencies, and (iii) to present the parametric study of natural frequency along with the related column parameters. In this paper, three differential equations were derived, which simultaneously governs free vibrations of the linear elastic tapered shear deformable column. The differential equation adopted in most studies in the open literature was derived as a fourth order differential equation only with respect to lateral deflection in terms of axial coordinates. To theoretically treat a tapered shear deformable column, it is too complex to remove the rotation terms caused by bending moment and shear force from equilibrium equations in dynamics based on Timoshenko beam theory. From this idea, the three differential equations with the total fourth-order, rather than one differential equations with a single fourth-order, decompose the deformation into lateral deflection, bending rotation, and shear deformation based on the work dealing with non-pre-stress beam problems (Lee et al., 2013).

The differential equations were numerically solved to compute the natural frequencies with mode shapes separately computed from the lateral deflection, bending rotation and shear deformation of the cross-section. To integrate differential equations, the Runge-Kutta method of the direct integration methods was applied, and to compute the natural frequencies, the determinant search method supplemented by the Regula-Falsi method was adopted. For this purpose, the two kinds of the linear and quadratic shape functions are chosen for which the solid square and circular cross-sections were applied. The three types of end conditions, most practical in the engineering fields, were considered, i.e., clamped-free, clamped-hinged and clamped-clamped. The first four natural frequencies with mode shapes were obtained. In calculating the amplitudes, the lateral deflection, angular rotation and shear deformation of the vibrating column were separately calculated. Through the parametric study, various effects on frequencies related to column parameters are extensively discussed.

2. Problem Formulation

2.1 Geometry of Column

Fig. 1(a) shows the geometry of a column with a length l vertically placed in the Cartesian coordinates (x, y) plane. The cross-section is square or circular with depth d at axial coordinate x, which is the length from the centroid of the square to the vertex and the radius of the circle, as shown in this figure. The volume V of the column is held in constant. The column is tapered under the condition of the constant volume, whose depth d varies along the axial coordinate x. The depth d at the bottom $(x = 0)$ is depicted as d_b and is denoted as d_t at the top $(x = l)$. At the coordinate x, the area and the moment inertia of plane area are denoted, respectively, as A and I. The column end is clamped at the bottom and is free or hinged or clamped at the top. Thus, the three end conditions of clamped-free, clamped-hinged and clamped-camped are combined in this study. Here, in presentations of the end condition, former stands for bottom end and latter stands for top end. The column acts externally to an axial load P from the top. When the column vibrates in the free state, the dynamic lateral deflection y occurs along the coordinate x. The shape of a vibrating deformed column axis, called the mode shape, is defined in Cartesian coordinates (x, y). Accordingly due to the lateral deflection y, the stress resultants in dynamics consisting of the axial force N, shear force Q and bending moment M occur along the axial coordinate x as shown in this figure. At coordinates (x, y), angular rotation caused by bending moment and shear deformation caused by shear force are depicted as θ and γ, respectively.

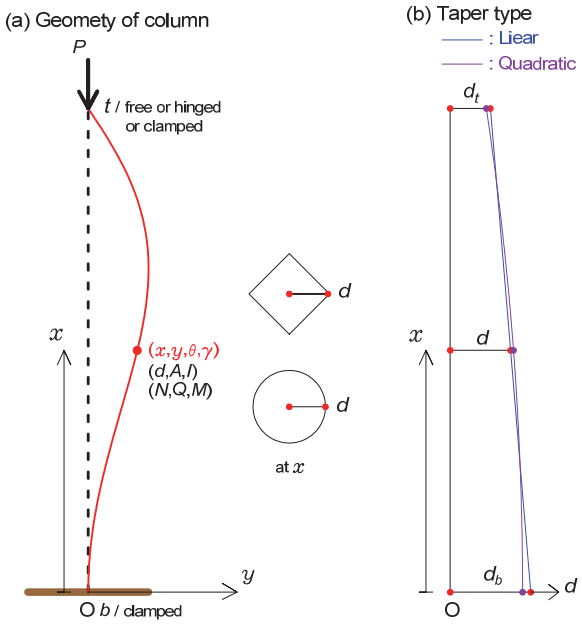

Fig. 1. (a) Geometry of column and its parameters and (b) Taper type under same volume

2.2 Cross-sectional Properties

The taper function d of the column is now defined. Although the function d is arbitrary, in this paper, the variation functions d are chosen as the linear and quadratic functions shown in Fig. 1(b) in terms of single variable x. To apply the taper function d, the taper ratio r of d_t to d_b is defined as

$$r = \frac{d_t}{d_b}. \tag{1}$$

When using Eq. (1), the taper function d at an axial coordinate x is given by

$$d = d_b F\left(\frac{x}{l}\right) = d_b F, \tag{2}$$

where the function $F = F(x/l)$ is as follows.

$$F = (r-1)\frac{x}{l} + 1 \text{ for linear taper} \tag{3.1}$$

$$F = (r-1)\left(\frac{x}{l}\right)^2 + 1 \text{ for quadratic taper} \tag{3.2}$$

Now, define the area A and the moment inertia of plane area I in terms of d at x for the square and circular cross-section., i.e.,

$$A = a_1 d^2 = a_1 d_b^2 F^2, \tag{4}$$

$$I = a_2 d^4 = a_2 d_b^4 F^4, \tag{5}$$

where the constants a_1 and a_2 are:

$$a_1 = 2,\ a_2 = \frac{1}{3} \text{ for square cross-section} \tag{6.1}$$

$$a_1 = \pi,\ a_2 = \frac{\pi}{4} \text{ for circular cross-section} \tag{6.2}$$

The constant volume V of the column material is obtained, or,

$$V = \int_0^l A dx = a_1 a_3 d_b^2 \, l \tag{7}$$

where the constant a_3 is:

$$a_3 = \frac{1}{3}(r^2 + r + 1) \text{ for linear taper} \tag{8.1}$$

$$a_3 = \frac{1}{15}(3r^2 + 4r + 8) \text{ for quadratic taper} \tag{8.2}$$

Using Eq. (7), A and I in Eq. (4) and Eq. (5) are rearranged as follows,

$$A = \frac{V}{a_3 l} F^2 \tag{9}$$

$$I = \frac{a_2 V^2}{a_1^2 a_3^2 l^2} F^4 \tag{10}$$

2.3 Governing Differential Equations

As mentioned above, the dynamic (N, Q, M) of the stress resultants caused by the deflection y act on the vibrating column. The lateral inertia force F_I due to y and rotary inertia couple R_I due to bending rotation are distributed along the column axis since the column has the mass. Fig. 2 shows an infinitely small element acting (N, Q, M) and (F_I, R_I) excited by kinetics of the free vibration. Here, the motion of free vibration assumes a harmonic motion from which dynamic coordinates are expressed in terms of $\sin(\omega_i t)$. For example, $y_{x,t} = y\sin(\omega_i t)$, where $y(= y_x)$ is the amplitude of the lateral deflection, ω_i is the ith angular frequency, and t is the time.

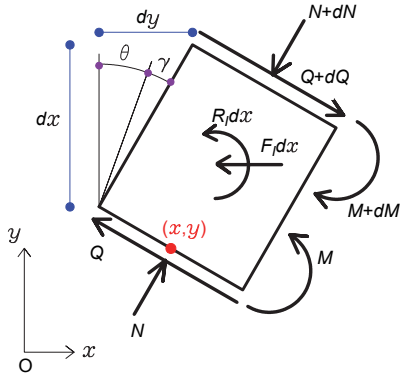

Fig. 2. Column element acting stress resultants and inertia forces

Considering equilibrium equations, $\sum F_y = 0$, $\sum M = 0$, in which the dynamics of (N, Q, M) and (F_I, R_I) are treated as the statics from the free body diagram in Fig. 2, these equations are arranged as follows,

$$\frac{dQ}{dx} - F_I = 0 \tag{11}$$

$$\frac{dM}{dx} + N\frac{dy}{dx} + Q - R_I = 0 \tag{12}$$

In Fig. 2, the slope dy/dx of the neutral axis of the deformed column is equal to the rotation of the cross-section consisting of angular rotation θ due to the bending moment M and shear deformation γ due to the shear force Q, that is

$$\frac{dy}{dx} = \theta + \gamma \tag{13}$$

The axial force N is equal to the applied compressive load P, that is

$$N = P \tag{14}$$

The relationships between load and strain are given by (Gere & Timoshenko, 1997)

$$Q = \alpha GA\gamma = \frac{\alpha GV}{a_3 l} F^2 \gamma, \tag{15}$$

$$M = EI\frac{d\theta}{dx} = \frac{a_2 V^2}{a_1^2 a_3^2 l^2} EF^4 \frac{d\theta}{dx}, \tag{16}$$

where E is the modulus of elasticity, G is the shear modulus of elasticity and α is the shear factor: $\alpha = 0.833$ for the square and $\alpha = 0.9$ for the circular cross-section.

The lateral inertia force F_I and the rotary inertia couple R_I are given by (Humar, 2002)

$$F_I = -\rho A\omega_i^2 y = -\frac{\rho V}{a_3 l}\omega_i^2 F^2 y \tag{17}$$

$$R_I = -\rho I\omega_i^2 \theta = -\frac{a_2 \rho V^2}{a_1^2 a_3^2 l^2}\omega_i^2 F^4 \theta \tag{18}$$

Using Eqs. (15) and (16), dQ/dx and dM/dx are obtained as

$$\frac{dQ}{dx} = \frac{\alpha GV}{a_3 l}\left[2F\frac{dF}{dx}\gamma + F^2\frac{d\gamma}{dx}\right] \tag{19}$$

$$\frac{dM}{dx} = \frac{a_2 V^2}{a_1^2 a_3^2 l^2} E\left[4F^3\frac{dF}{dx}\frac{d\theta}{dx} + F^4\frac{d^2\theta}{dx^2}\right] \tag{20}$$

To derive the non-dimensional differential equations, the non-dimensional system parameters are defined as follows,

$$\xi = \frac{x}{l} \tag{21}$$

$$\eta = \frac{y}{l} \tag{22}$$

$$\lambda = \frac{V}{l^3} \tag{23}$$

$$\mu = \frac{G}{E} \tag{24}$$

$$p = \frac{Pl^4}{EV^2} \tag{25}$$

$$C_i = \omega_i l\sqrt{\frac{\rho}{E}} \tag{26}$$

where (ξ, η) are the non-dimensional Cartesian coordinates, λ is the volume ratio, μ is the elasticity ratio, p is the load parameter and C_i is the frequency parameter.

Using Eqs. (21)-(26), Eqs. (11)-(13) are converted into nondimensional differential equations. First, the expression in the non-dimensional form of Eq. (13) becomes Eq. (27). Second, Eqs. (14), (15), (18) and (20) are substituted into Eq. (12) and then the non-dimensional differential Eq. (28) is obtained. Finally, Eqs. (17) and (19) are substituted into Eq. (12) and then the non-dimensional differential Eq. (29) is yielded:

$$\frac{d\eta}{d\xi} = \theta + \gamma \tag{27}$$

$$\frac{d^2\theta}{d\xi^2} = -\frac{a_1^2 a_3^2}{a_2}\frac{p}{f^4}\frac{d\eta}{d\xi} - \frac{4}{f}\frac{df}{d\xi}\frac{d\theta}{d\xi} - C_i^2\theta - \frac{a_1^2 a_3}{a_2}\frac{\alpha\mu}{\lambda}\frac{\gamma}{f^2} \tag{28}$$

$$\frac{d\gamma}{d\xi} = -\frac{C_i^2}{\alpha\mu}\eta - \frac{2}{f}\frac{df}{d\xi}\gamma \tag{29}$$

where f and $df/d\xi$ are

$$f = (r-1)\xi + 1;\ \frac{df}{d\xi} = r - 1 \text{ for linear taper} \tag{30.1}$$

$$f = (r-1)\xi^2 + 1;\ \frac{df}{d\xi} = 2(r-1)\xi \text{ for quadratic taper} \tag{30.2}$$

Now, the boundary conditions of the column are considered. The bottom end ($x = 0$) is clamped in which the deflection y and the slope dy/dx ($= \theta + \gamma$) are zero. Its boundary conditions in dimensionless forms are

$$\eta = 0,\ \theta + \gamma = 0 \text{ at clamped end } (\xi = 0) \tag{31}$$

The top end ($x = l$) is free or hinged or clamped. At the free end, the bending moment M in Eq. (16) and the shear force Q in Eq. (15) are zero. Its dimensionless boundary conditions become

$$\frac{d\theta}{d\xi} = 0,\ \gamma = 0 \text{ at free end } (\xi = 1) \tag{32}$$

At the hinged end, the deflection y and the bending moment M are zero. Its dimensionless boundary conditions are

$$\eta = 0,\ \frac{d\theta}{d\xi} = 0 \text{ at hinged end } (\xi = 1) \tag{33}$$

At the clamped end, the deflection y and the slope dy/dx are zero. Its dimensionless boundary conditions become

$$\eta = 0,\ \theta + \gamma = 0 \text{ at clamped end } (\xi = 1) \tag{34}$$

3. Numerical Method and Validation

Based on the mathematical formulation developed herein, a FORTRAN computer program was coded to compute the frequency parameter C_i with mode shapes $(\xi, \eta)_i$. The columns with clamped-free, clamped-hinged and clamped-clamped end conditions were considered for a given column parameters: cross-sectional shape (square or circular), taper type (linear or quadratic), taper ratio r, elasticity ratio μ, volume ratio λ and load parameter p. The 4th order differential equations, Eqs. (27)-(29), were numerically solved using the trial eigenvalue method. To integrate differential equations, the Runge-Kutta method (Burden et al., 2016) of the direct integral method was adopted, and to obtain frequency parameter C_i, the determinant search method supplemented by the Regula-Falsi method (Burden et al., 2016) was used. Interesting readers can refer to a paper detailing such a numerical method (Lee et al., 2013). The four lowest angular frequencies ω_i in rad/s obtained from this study were compared to those from Karnovsky and Lebed (2000) in Table 1. The column parameters in the dimensional forms were square cross-section, linear taper, $l = 3$m, $d_a = d_b = 0.2$m, $E = 210$GPa, $G = 80$GPa, $\rho = 7850$kg/m^3 and $P = 3$MN. Since the results of Karnovsky and Lebed did not consider the rotary inertia

and shear deformation, the results of this study also did not consider these effects. From the value C_i predicted in this study, ω_i was calculated by Eq. (26) as $\omega_i = (C_i/l\sqrt{E/\rho}) = 1724.1C_i$ rad/s. Each angular frequency ω_i of this study and reference was very well matched to each other with an average error of 0.15% within 0.65% error. The frequencies compared in Table 1 verify the adequacy of the theories and solution methods developed in this study.

Table 1. Angular frequencies ω_i of this study and Karnovsky and Lebed (2000)

		Angular frequency ω_i in rad/s			
End condition	Data source	$i=1$	$i=2$	$i=3$	$i=4$
Clamped-free	This study	156.54	1024.9	2888.7	5671.5
	Karnovsky	157.27	1025.6	2887.9	5666.4
Clamped-hinged	This study	718.95	2340.2	4890.4	8371.8
	Karnovsky	719.23	2339.6	4886.5	8359.7
Clamped-clamped	This study	1046.7	2890.9	5674.0	9388.3
	Karnovsky	1040.4	2890.2	5668.5	9373.2

* See text for the column parameters.

4. Parametric Study and Discussion

Using the computer code written in this study, the parametric study of the frequency parameter C_i and its discussion were performed, and the results are shown in Tables 2-5 and Figs. 3-6. For the first parametric study of four lowest C_i ($i = 1,2,3,4$), the effects of rotary inertia indexed with E_R and shear deformation indexed with E_S were performed and shown in Table 2, where column parameters are given at the bottom. Because the rotary inertia couple R_I originated from Eq. (18) is related to the term $C_i\theta$ in Eq. (22), if R_I is excluded, i.e. $E_R = 0$, this term can simply be deleted from Eq. (28) and if included, i.e. $E_R = 1$, this term is remained in Eq. (28). The shear rigidity GA becomes ∞ (Humar, 2002) if the shear deformation is excluded, i.e. $E_s = 0$. Thus, to satisfy this necessary, a very large value of $\mu(= G/E)$ was considered in the differential equations, Eqs. (28) and (29), if $E_s = 0$. Even though $\mu = \infty$ was applied to these equations, the differential equation systems correctly worked. This is because that Eqs. (28) and (29) are internally correlated with each other, and differential equations with $\mu = \infty$, i.e. $1/\infty = 0$, remain valid. It is well-known that in the ordinary beam, the index is $E_R = E_S = 0$ and in the Timoshenko beam, the index is $E_R = E_S = 1$. It is observed that the rotary inertia and shear deformation depresses values of C_i. This is because these effects increase the deformation of y, θ and γ thus lowering the natural frequency when the beam vibrates at the same energy. These two effects are greater for higher mode than lower mode. For example, the Timoshenko beam to ordinary beam ratios of C_i with the clamped-clamped column increase in order from 1.0089(=0.6009/0.5956) to 1.0216 to 1.0412 to 1.0678 as increasing $i = 1,2,3,4$. When calculating C_i in high mode, the two effects cannot be ignored, especially for the columns excited by higher frequencies.

Table 2. Effects of rotary inertia (E_R) and shear deformation (E_S) on frequency parameter C_i

			Frequency parameter C_i			
End condition	E_R	E_S	$i=1$	$i=2$	$i=3$	$i=4$
Clamped-free	0	0	0.0882	0.6512	1.7639	3.4122
	1	0	0.0880	0.6411	1.7184	3.2524
	1	1	0.0876	0.6417	1.7123	3.2412
Clamped-hinged	0	0	0.4507	1.4056	2.9095	4.9609
	1	0	0.4487	1.3833	2.8116	4.6782
	1	1	0.4470	1.3782	2.8016	4.6623
Clamped-clamped	0	0	0.6009	1.6806	3.3169	5.5028
	1	0	0.5978	1.6511	3.1968	5.1709
	1	1	0.5956	1.6451	3.1855	5.1535

* Column parameters: square, linear, $r = 0.5,\ \mu = 0.38,\ \lambda = 0.01$ and $p = 0.2$

Table 3 compares the frequency parameters C_i of the square and circular sections, where column parameters are at the bottom. As expected, the values C_i of square shape are larger than those of circular shape in all cases. Same results for the buckling load problems had been reported in the work (Gere and Timoshenko, 1997). For the clamped-free column, the value C_i of square shape is 12.16%(0.0876/0.0781=1.1216) greater than that of circular shape for $i = 1$ and 2.20% greater for $i = 4$. From this table, it can be seen that the cross-sectional shape has a greater effect in the lower mode than in the higher mode.

Table 3. Comparison of frequency parameter C_i between square and circular cross-section

		Frequency parameter C_i			
End condition	Cross-section	$i = 1$	$i = 2$	$i = 3$	$i = 4$
Clamped-free	Square	0.0876	0.6417	1.7123	3.2412
	Circular	0.0781	0.6231	1.6719	3.1713
Clamped-hinged	Square	0.4476	1.3782	2.8016	4.6623
	Circular	0.4352	1.3461	2.7405	4.5665
Clamped-clamped	Square	0.5956	1.6452	3.1855	5.1535
	Circular	0.5812	1.6077	3.1170	5.0488

* Column parameters: linear, $r = 0.5,\ \mu = 0.38,\ \lambda = 0.01, p = 0.2$ and $E_R = E_S = 1$

Table 4 compares the frequency parameters C_i of the linear and quadratic tapers, where column parameters are at the bottom. The effects of taper type depend on the end conditions. For the columns with clamped-hinged and clamped-clamped end conditions, the value C_i of the linear taper is greater than the value of the quadratic taper, but the opposite is true for the clamped-free column. For the clamped-clamped column with $i = 1$, C_i of the linear taper is 8.52% (0.5956/0.5488=1.0852) greater than that of quadratic taper, implying that the taper effect cannot be ignored. These results show that choosing the proper taper type can improve the robustness of the column in dynamic behavior.

Table 4. Comparison of frequency parameter C_i between linear and quadratic taper

		Frequency parameter C_i			
End condition	Taper type	$i = 1$	$i = 2$	$i = 3$	$i = 4$
Clamped-free	Linear	0.0876	0.6417	1.7123	3.2412
	Quadratic	0.0921	0.6559	1.7322	3.2691
Clamped-hinged	Linear	0.4476	1.3782	2.8016	4.6623
	Quadratic	0.4235	1.3505	2.7794	4.6466
Clamped-clamped	Linear	0.5956	1.6452	3.1855	5.1535
	Quadratic	0.5488	1.5852	3.1263	5.0980

* Column parameters: square, $r = 0.5,\ \mu = 0.38,\ \lambda = 0.01, p = 0.2$ and $E_R = E_S = 1$

Table 5. Effect of elasticity ratio μ on frequency parameter C_i

		Frequency parameter C_i			
End condition	μ	$i = 1$	$i = 2$	$i = 3$	$i = 4$
Clamped-free	0.333	0.0876	0.6414	1.7114	3.2396
	0.35	0.0876	0.6415	1.7117	3.2402
	0.4	0.0877	0.6419	1.1726	3.2417
	0.5	0.0877	0.6423	1.7137	3.2498
Clamped-hinged	0.333	0.4467	1.3775	2.8002	4.6601
	0.35	0.4468	1.3778	2.8007	4.6609
	0.4	0.4471	1.3785	2.8021	4.6631
	0.5	0.4474	1.7995	2.8040	4.6735
Clamped-clamped	0.333	0.5953	1.6442	3.1839	5.1511
	0.35	0.5954	1.6446	3.1845	5.1520
	0.4	0.5957	1.6454	3.1861	5.1544
	0.5	0.5961	1.6465	3.1882	5.1677

* Column parameters: square, linear, $r = 0.5,\ \lambda = 0.01,\ p = 0.2$ and $E_R = E_S = 1$

Table 5 shows the effects of elasticity ratio $\mu(=G/E)$ on the frequency parameter C_i, where the column parameters are at the bottom. The value μ varies from 1/3 to 1/2, which is the actual range of the structural materials and it is noted that $\mu = 0.5$ is the largest theoretical value. The value C_i increases with increasing μ, implying that the high shear stiffness performs robustness from the dynamic behaviors. The effect of μ is more dominant for higher modes: for example, the ratio C_i of $\mu = 0.5$ to $\mu = 0.333$ is 1.0011(0.0877/0.876=1.0011) for clamped-free column with $i = 1$, but its ratio with $i = 4$ is 1.0031.

In the following numerical examples of Fig. 3-5, first frequency parameters $C_{i=1}$ are only represented and discussed since the first natural frequency is most useful in the practical engineering fields (Carpinteri et al., 2014). Fig. 3 shows the frequency curves indicating the relationship between the taper ratio r and the first frequency parameter C_1 for the clamped-free, clamped-hinged and clamped-clamped columns. The column parameters are given at the top of this figure. As r increases, the value C_1 increases and reaches the peak coordinates and decreases. For clamped-free column, the peak, i.e. maximum, coordinates occur at (0.441,0.0906), marked by ▲, which means that at taper ratio $r = 0.441$, the maximum value $C_1 = 0.0906$ is achieved. This taper ratio, defied by r_{opt}, is known as the dynamic optimal taper ratio with maximum frequency under the condition of same column volume (Lee et al., 2012). The other two columns also have maximum coordinates marked by ▲. Also, for the clamped-free column, it is observed that at two ends of $r = 0.311$ and $r = 1.034$ marked by ■, the value C_1 vanish, i.e. $C_1 = 0$, and then the column buckles. Therefore, in the region of $r \leq 0.312$ and $r \geq 1.034$, the column is buckled for the applied load $p = 0.2$ and consequently, the column is stable in the region of $0.312 < r < 1.034$ for $p = 0.2$. For the columns with clamped-hinged and clamped-clamped end conditions, the stable regions also exist. In this case, the minimum stable taper ratios marked by ■ are presented but the maximum stable taper ratios are not presented in this figure, which are located outside $r = 1.5$.

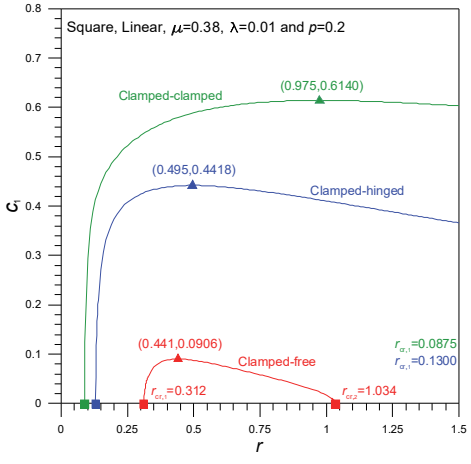

Fig. 3. r versus C_1 curves

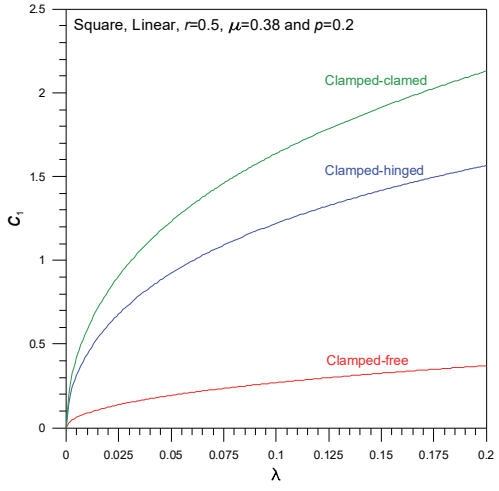

Fig. 4. λ versus C_1 curves

The relationship between the volume ratio λ and the first frequency parameter C_1 is presented in Fig. 4, in which the column parameters are given at the top. As expected, the value C_1 increases with increasing λ. The increasing rate of C_1 decreases with increasing λ.

Fig. 5 shows the frequency curves for the first frequency parameter C_1 and the load parameter p, where the column parameters are given at the top. The C_1 decreases as p increases, and finally, C_1 become zero at the buckling load parameters $p(=p_{cr})$, i.e., at the coordinates $(0, p_{cr})$ marked by ■, respectively. From these frequency curves, the buckling load parameters p_{cr} can be determined. For example, p_{cr} of the clamped-free column for a given column parameters is $p_{cr} = 0.2527$ marked by ■ in the p axis.

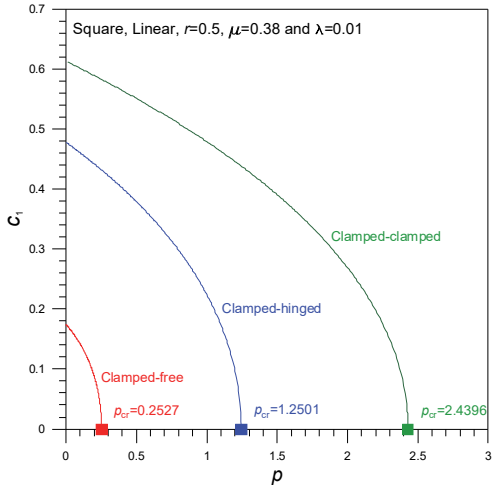

Fig. 5. p versus C_1 curves

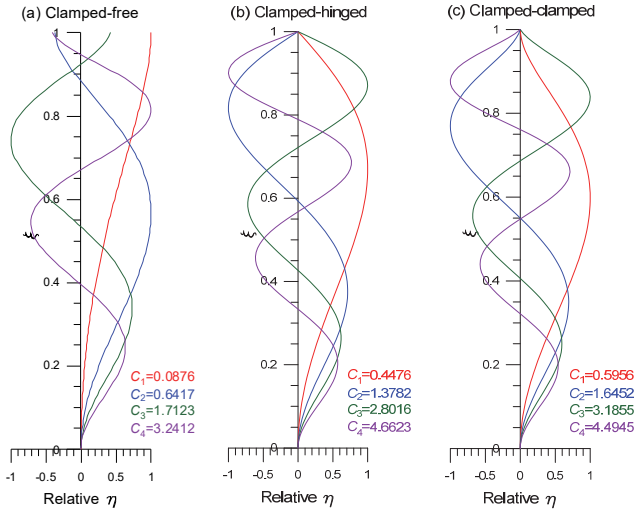

Fig. 6. Examples of mode shape for square, linear, $r = 0.5$, $\mu = 0.38$, $\lambda = 0.01$, $p = 0.2$ and $E_R = E_S = 1$

The typical examples of the mode shape are shown in Fig. 6 whose column parameters are square, linear, $r = 0.5$, $\mu = 0.38$, $\lambda = 0.01$ and $p = 0.2$. From these mode shapes, locations of nodal points and maximum deflections of the buckled columns are fully understood, which are one of the most useful data for the stability analysis and structural design.

5. Concluding Remarks

In this paper, the free vibrations of the tapered shear deformable column were studied. The cross-section of the column with the constant volume was square or circular, and the taper function was linear or quadratic. In parametric study, three end conditions of the clamped-free, clamped-hinged and clamped-clamped were considered. The total fourth order three differential equations governing free vibrations of such column were derived based on the Timoshenko beam theory using deformation decompositions consisting of the lateral deflection, bending rotation and shear deformation.

The differential equations were numerically solved to compute the natural frequencies with mode shapes. To integrate the differential equations, the fourth order Runge-Kutta method was applied and to calculate the natural frequencies, the determinant search method supplemented by the Regula-Falsi method was adopted. For the validation purpose, angular frequencies obtained from this paper and Karnovsky and Lebed (2000) were compared for the uniform columns. Through the FORTRAN computer program written in this study, the parametric studies of the natural frequency with the mode shape were performed, and its results were extensively discussed.

The buckling load problem for a tapered shear deformable column using deformation decomposition based on the theory of this study is needed for further study.

Acknowledgments

This study was funded by the Wonkwang University Research Fund in 2019. The corresponding author, G. S. Kim, thanks for this support.

References

Andrade, A., Camotim, D., & Dinis, P. B. (2007). Lateral-torsional buckling of singly symmetric web-tapered thin-walled I-beams: 1D model vs. shell FEA. *Computers & Structures*, *85*(17-18), 1343-1359.

Burden, R. L., Faires, D. J. & Burden, A. M. (2016). *Numerical Analysis*. Cengage Learning, MA, USA.

Carpinteri, A., Malvano, R., Manuello, A., & Piana, G. (2014). Fundamental frequency evolution in slender beams subjected to imposed axial displacements. *Journal of Sound and Vibration*, *333*(11), 2390-2403.

Gere, J. M. &Timoshenko, S. P. (1997). *Mechanics of Materials*. PWS Publishing Company, MA, USA.

Humar, J. L. (2002). *Dynamics of Structures*. A. A. Balkema Publisher, Rotterdam, Netherlands.

Karnovsky, I. A. & Lebed, O. I. (2000). *Formulas for Structural Dynamics*. McGraw Hill, NY, USA.

Lee, B. K., Oh, S. J., & Lee, T. E. (2013). Free vibration of tapered Timoshenko beams by deformation decomposition. *International Journal of Structural Stability and Dynamics*, *13*(02), 1250057.

Lee, B. K., Lee, T. E., Choi, J. M., & Oh, S. J. (2012). Dynamic optimal arches with constant volume. *International Journal of Structural Stability and Dynamics*, *12*(06), 1250044.

Lee, J. K. & Lee, B. K. (2020). Buckling optimization of axially functionally graded columns with constant volume. Engineering Optimization (under review).

Li, G. Q. & Li, J. J. (2002). A tapered Timoshenko-Euler beam element for analysis steel portal frame. *Journal of Computational Steel Research, 58*, 1531-1544.

Loya, J. A., Rubio, L., & Fernández-Sáez, J. (2006). Natural frequencies for bending vibrations of Timoshenko cracked beams. *Journal of Sound and Vibration*, *290*(3-5), 640-653.

Maalek, S. (1999). Shear defection of Tapered Timoshenko beams. *International Journal of Mechanical Science, 46*, 783-805.

Shimpi, R. P., Shetty, R A. & Guha, A. (2017). A simple single variable shear deformation theory for a rectangular beam. *Journal of Mechanical Engineering Science, 231*(24), 4576-4591.

Takahashi, I. (1999). Vibration and stability of non-uniform cracked Timoshenko beam subjected to follower force. *Computational Structure, 71*, 585-591.

Timoshenko, S. P. & Young, D. H. (1974). *Vibration Problems in Engineering*. John Wiley and Sons, NJ, USA.

Viola, E., Ricci, P., & Aliabadi, M. H. (2007). Free vibration analysis of axially loaded cracked Timoshenko beam structures using the dynamic stiffness method. *Journal of Sound and Vibration*, *304*(1-2), 124-153.

Yang, Y. B., & Yau, J. D. (1987). Stability of beams with tapered I-sections. *Journal of Engineering Mechanics*, *113*(9), 1337-1357.

Yardimoglu, B., & Yildirim, T. (2004). Finite element model for vibration analysis of pre-twisted Timoshenko beam. *Journal of Sound and Vibration*, *273*(4-5), 741-754.

Yau, J. D. (2006). Stability of tapered I-beams under torsional moments. *Finite Elements in Analysis and Design*, *42*(10), 914-927.

Zhou, D. (2001). Free vibration of multi-span Timoshenko beams using static Timoshenko beam functions. *Journal of Sound and Vibration*, *241*(4), 725-734.